

ELECTROMAGNETIC SCATTERING FROM COATED STRIPS UTILIZING THE ADAPTIVE MULTISCALE MOMENT METHOD

C. Su

Dept. of Applied Math.
Northwestern Polytechnical University
Xian, Shaanxi, P. R. China

T. K. Sarkar

Department of Electrical and Computer Engineering
Syracuse University
Syracuse, NY 13244-1240, USA

- 1. Introduction**
- 2. The Basic Formulation**
- 3. The Computational Formula of the Moment Method for a Multiscale Basis**
 - 3.1 Multiscale Basis Functions
 - 3.2 Transverse Electric (TE) Case
 - 3.3 Transverse Magnetic (TM) Case
- 4. Adaptive Algorithm for Linear Equations Using the Multiscale Basis**
- 5. Numerical Results**
- 6. Conclusion**
- Acknowledgment**
- References**

1. INTRODUCTION

Coated conductors have recently been used either to protect the conducting surface from the environment or to reduce the radar cross

section. The electromagnetic scattering from finite coated conducting surfaces have been extensively studied. Various numerical techniques and formulations have been used. The most commonly used approach is the method of moment [1]. However, this approach is computationally intensive and is unsuitable for solving electrically large coated surfaces.

Medgyesi-Mitschang, Putnam and Wang [2, 3] proposed the moment method with an entire domain Galerkin basis for the solution of a coupled system of electric- and magnetic-field integral equations to study the EM scattering from electrically large coated flat and curved strips. Kishk et al. [4] presented the formulation for the coated conductor of the three-dimensional bodies of revolution based on existing E-PMCHW formulation. This formulation is valid both for thick coatings and for coating thickness that approaches zero. Petre et al. [5, 6] have studied the scattering from one-dimensional periodic coated strips, in which the integral equations were formulated in the spectral domain using the Fourier transform of the integrodifferential equations due to the periodicity of the structure. The generalized biconjugate gradient-Fast Fourier transform (Bi CG-FFT) method with subdomain basis functions were applied to solve the EFIE, MEIE and CFIE equations. Rao et al [7] formulated in terms of a set of the couple integral equations involving equivalent electric and magnetic surface currents in order to analyze the electromagnetic field scattered by arbitrarily shaped, three-dimensional conducting objects coated with lossy dielectric materials of arbitrarily thickness. The conducting structures and dielectric materials are approximated by planar triangular patches and the moment method is used to solve the integral equations.

Proper choice of basis functions is important for the moment method. The basis functions commonly used in solving antenna and scattering problems are of two types: entire domain functions and subdomain functions. The typical entire domain basis functions are Fourier (sine and cosine) functions, Chebychev polynomial functions, Legendre, Hermite, Maclaaurin polynomial functions [8, 9]. Typical subdomain basis functions are pulse, piecewise linear (triangular) functions, piecewise sinusoidal functions etc. [10, 11].

Recently, a new kind of subdomain basis functions have been introduced, that is, the wavelet basis and wavelet-like basis. They have been applied successfully in many engineering disciplines [12–17]. They have also been used to analyze electromagnetic scattering problems [18–24].

A specially tailored wavlet-like basis has also been used for efficient solution of the differential form of Maxwell's equations [25, 26]. Because the wavelet basis and wavelet-like basis have local supports and vanishing moment properties, the system matrix constructed by the moment method can be formed as a sparse matrix by filtering many of the relatively small elements of the matrix through the introduction of a suitable threshold. This means that one can save CPU-time and reduce the storage for the solution of matrix equations.

The method of non-uniform grid and the multiscale technique which generates locally finer grid are usually used when the solutions of the integral equations or the differential equations has been known to vary widely in different domains. By non-uniform gridding one can reduce the size of the problem and improve the accuracy. The multilevel or the multigrid technique has been widely used in solving the differential equations and integral equations [27–31]. Kalbasi and Demarest [32, 33] applied the multilevel concepts to solve the integral equation by the moment method on different levels, which has been called the multilevel moment method. No matter what the multigrid technique is, the basis functions for an improved approximation have to be reconstructed again. By using the multiscale technique in one dimension, the basis functions for the new scale have to be reconstructed. Although for the new approximation grids formed by the multiscale technique is the same as that for the multilevel technique, however the construction of the functions are different.

The aim of this paper is to consider the problem of electromagnetic scattering from perfectly conducting strips coated with thin dielectric material by use of the adaptive multiscale moment method (AMMM). In the next section, the basic formulation is presented for analysis of scattering from coated conducting strips on the basis of a coupled system of electric- and magnetic-field integral equations. Section 3 outlines the computational methodology of the multiscale basis by use of the moment method. Section 4 presents AMMM to solve the coupled EM integral equations. Section 5 presents a variety of numerical examples for different coating strips followed by conclusion.

2. THE BASIC FORMULATION

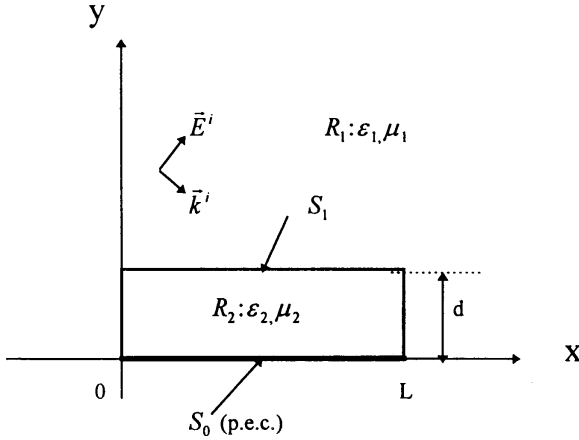


Figure 1. Geometry of a coated flat strip L width with E-polarized incident wave

Consider a time-harmonic electromagnetic wave (\vec{E}^i, \vec{H}^i) incident on an infinite thin, perfectly conducting strip coated with a homogeneous dielectric material as shown in Fig. 1. The permittivity and permeability of the coating (ϵ_2, μ_2) can be complex. We assume that the strip width is larger than the thickness of the coating, i.e., $d \ll L$.

The total electrical and magnetic field in the region R_1 , at a field point \vec{r} can be represented by the following coupled system of integrodifferential equations

$$\begin{cases} \theta(\vec{r})\vec{E}_1(\vec{r}) = \vec{E}^i(\vec{r}) - L_1\vec{J}_1^+(\vec{r}) + K_1\vec{M}_1^+(\vec{r}) - L_1\vec{J}_0^-(\vec{r}) \\ \theta(\vec{r})\vec{H}_1(\vec{r}) = \vec{H}^i(\vec{r}) - K_1\vec{J}_1^+(\vec{r}) - \frac{1}{\eta_1^2}L_1\vec{M}_1^+(\vec{r}) - K_1\vec{J}_0^-(\vec{r}) \end{cases} \quad (1)$$

where $\eta_1 = \sqrt{\frac{\mu_1}{\epsilon_1}}$ and $\vec{J}_0^+(\vec{r})$, $\vec{J}_0^-(\vec{r})$ are the equivalent electric surface current defined on the upper and lower surface of S_0 , $\vec{J}_1^\pm(\vec{r})$, $\vec{M}_1^\pm(\vec{r})$ are the equivalent electric and magnetic currents defined on the upper and lower surface of S_1 , where $\vec{J}_1^+(\vec{r}) = -\vec{J}_1^-(\vec{r})$ and $\vec{M}_1^+(\vec{r}) = -\vec{M}_1^-(\vec{r})$.

The fields in the region R_2 are expressed as:

$$\begin{cases} \theta(\vec{r})\vec{E}_2(\vec{r}) = -L_2\vec{J}_1^-(\vec{r}) + K_2\vec{M}_1^-(\vec{r}) - L_2\vec{J}_0^+(\vec{r}) \\ \theta(\vec{r})\vec{H}_2(\vec{r}) = -K_2\vec{J}_1^-(\vec{r}) - \frac{1}{\eta_2^2}L_2\vec{M}_1^-(\vec{r}) - K_2\vec{J}_0^+(\vec{r}) \end{cases} \quad (2)$$

The integrodifferential operators L_i, K_i in the equations (1) and (2) are defined as

$$\begin{cases} L_i\vec{X}(\vec{r}) = jk_i\eta_i \int_{\partial R_i} (\vec{X}(\vec{r}') + k_i^{-2}\nabla\nabla' \cdot \vec{X}(\vec{r}'))\Phi(k_i|\vec{r} - \vec{r}'|)ds' \\ K_i\vec{X}(\vec{r}) = \int_{\partial R_i} \vec{X}(\vec{r}') \times \nabla\Phi(k_i|\vec{r} - \vec{r}'|)ds' \end{cases} \quad (3)$$

where $\Phi(k_it) = \frac{1}{4j}H_0^{(2)}(k_it)$, $k_i = \frac{2\pi}{\lambda_i}$, $\theta(\vec{r})$ is defined as

$$\theta(\vec{r}) = \begin{cases} 1 & \vec{r} \in R_i \\ 1/2 & \vec{r} \in \partial R_i \\ 0 & \text{otherwise} \end{cases}$$

and ∂R_i is the boundary of the region R_i .

By use of the boundary condition (that is, the tangential components of the total fields are continuous on S_1 , and the tangential components of the total electric field is zero on the perfectly conducting surface), the basic integrodifferential equations can be obtained:

$$\vec{E}^i(\vec{r})\Big|_{tan} = \left\{ (L_1 + L_2)\vec{J}_1(\vec{r}) - (K_1 + K_2)\vec{M}_1(\vec{r}) + L_1\vec{J}_0^-(\vec{r}) - L_2\vec{J}_0^+(\vec{r}) \right\}\Big|_{tan} \quad \vec{r} \in S_1 \quad (4a)$$

$$\vec{H}^i(\vec{r})\Big|_{tan} = \left\{ (K_1 + K_2)\vec{J}_1(\vec{r}) - \left(\frac{1}{\eta_1^2}L_1 + \frac{1}{\eta_2^2}K_2\right)\vec{M}_1(\vec{r}) + K_1\vec{J}_0^-(\vec{r}) - K_2\vec{J}_0^+(\vec{r}) \right\}\Big|_{tan} \quad \vec{r} \in S_1 \quad (4b)$$

$$\vec{E}^i(\vec{r})\Big|_{tan} = \left\{ L_1\vec{J}_1(\vec{r}) - K_1\vec{M}_1(\vec{r}) + L_1\vec{J}_0^-(\vec{r}) \right\}\Big|_{tan} \quad \vec{r} \in S_1^- \quad (4c)$$

$$0 = \left\{ -L_2\vec{J}_1(\vec{r}) + K_2\vec{M}_1(\vec{r}) + L_2\vec{J}_0^+(\vec{r}) \right\}\Big|_{tan} \quad \vec{r} \in S_1^+ \quad (4d)$$

where $\vec{J}_1(\vec{r}) = \vec{J}_1^+(\vec{r})$ and $\vec{M}_1(\vec{r}) = \vec{M}_1^+(\vec{r})$. The equivalent currents across the edges of the coating are neglected.

Our goal is to analyze the electromagnetic scattering from the coated flat strip, that is, to solve the above coupled integral equations by the adaptive multiscale moment method and to compute the scattering fields.

3. THE COMPUTATIONAL FORMULA OF THE MOMENT METHOD FOR A MULTISCALE BASIS

3.1 Multiscale Basis functions

The triangular basis functions on a uniform grid on the interval $[0, L]$ with $N + 1$ nodes can be noted as

$$\begin{aligned}\phi_{0,0}(x) &= \Lambda(x) \\ \phi_{0,N}(x) &= \Lambda(x - L) \\ \phi_{0,i}(x) &= \Lambda(x - x_{0,i}) \quad i = 1, 2, \dots, N - 1\end{aligned}\tag{5}$$

where $x_{0,i} = \frac{iL}{N} = ih$; $i = 0, 1, 2, \dots, N$, $h = L/N$

$$\Lambda(x) = \begin{cases} 1 - \frac{x}{h} & \text{for } 0 < x < h \\ 1 + \frac{x}{h} & \text{for } -h < x < 0 \end{cases}$$

By multiscale in the interval $[0, L]$, the new increasing nodes are located at

$$x_{1,i} = \frac{x_{0,i-1} + x_{0,i}}{2} = (i - \frac{1}{2})h$$

and the improved basis functions are

$$\phi_{1,i}(x) = \Lambda[2(x - x_{1,i})]\tag{6}$$

By increasing the scale V -times in the interval $[0, L]$, the newly developed nodes are located at

$$x_{V,i} = \left(\frac{1}{2^V} + \frac{i-1}{2^{V-1}} \right) h, \quad i = 1, 2, \dots, 2^{V-1}N\tag{7}$$

and the new basis functions are

$$\phi_{V,i}(x) = \Lambda[2^V(x - x_{V,i})]\tag{8}$$

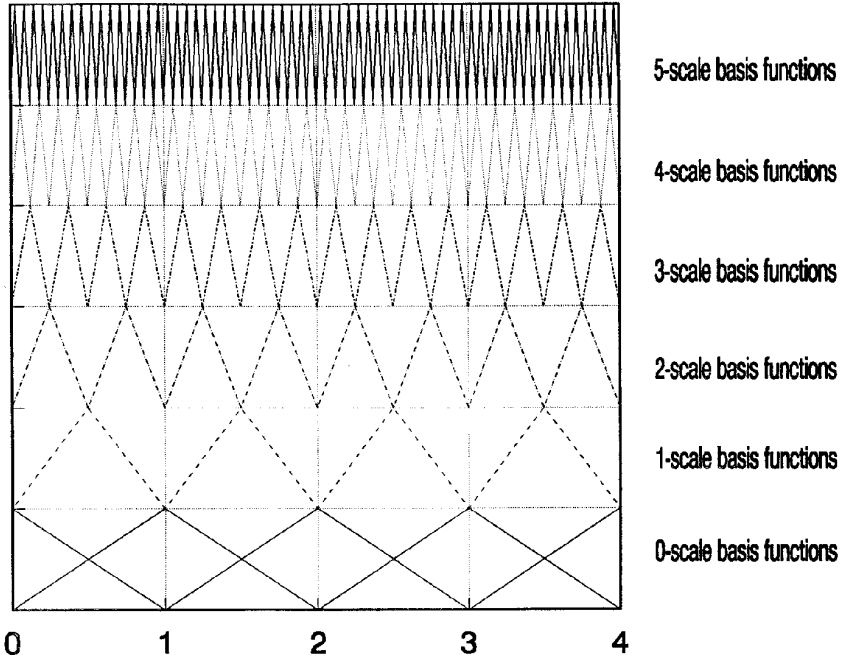


Figure 2. Basis functions on different scales for $N = 4$

$\{\phi_{V,i}(x)\}$ are referred to as the V -times multiscale basis functions which have a compact support. Specially, the 0-times multiscale basis functions is the ordinary triangular basis functions.

The multiscale basis functions are shown in Fig. 2 for the case of $N = 4$, $L = 4$, and $V = 5$ in the interval $[0, 4]$. $\Lambda(x)$ is different for the mother wavelet in wavelet analysis, which does not have the vanish moment property. The basis functions $\{\phi_{V,i}(x)\}$ on $[0, L]$ can be constructed by means of the shifting and dilating the function $\Lambda(x)$. The derivative of $\Lambda(x)$ is similar to the Haar wavelet.

For any piecewise continuous function $f(x)$ on $[0, L]$, the V 'th approximation function $f_V(x)$ is represented by

$$\begin{aligned}
 f_V(x) &= f_{V-1}(x) + \sum_{i=1}^{2^{V-1}N} \tau_{V,i} \phi_{V,i}(x) \\
 &= \sum_{i=0}^N \tau_{0,i} \phi_{0,i}(x) + \sum_{j=1}^V \sum_{i=1}^{2^{j-1}N} \tau_{j,i} \phi_{j,i}(x)
 \end{aligned} \tag{9}$$

where

$$\tau_{V,i} = f(x_{V,i}) - \frac{1}{2} \left(f(x_{V,i} - \frac{1}{2V}h) + f(x_{V,i} + \frac{1}{2V}h) \right)$$

This means that $\tau_{V,i}$ is the second-order central difference of $f(x)$ at $x_{V,i}$ on the interval $[x_{V,i} - \frac{h}{2V}, x_{V,i} + \frac{h}{2V}]$.

If $f(x)$ possesses the second-order differentiability condition at $x_{V,i}$, then

$$\tau_{V,i} \approx -\frac{h^2}{2V+2} f''(x_{V,i}) \quad (10)$$

If $|\tau_{j,i}| \leq \varepsilon$ (ε is the given threshold), $\tau_{j,i}$ can be set to zero.

Suppose $f(x)$ is the original function, $f_{tria}(x)$ is the approximation function utilizing the triangular basis functions. $f_{multi}(x)$ is the approximation obtained through the use of the multiscale triangular basis functions on V -scale neglecting the smaller terms.

$$\begin{aligned} \|f(x) - f_{multi}(x)\| &\equiv \int_0^L |f(x) - f_{multi}(x)| dx \\ &\leq \|f(x) - f_{tria}(x)\| + \|f_{tria}(x) - f_{multi}(x)\| \\ &\leq \|f(x) - f_{tria}(x)\| + \sum_{v=1}^V \int_0^L \varepsilon n_v |\Lambda(2^v x)| dx \\ &\leq \|f(x) - f_{tria}(x)\| + \varepsilon V \end{aligned}$$

where n_v is the number of the neglected terms for the V -scale.

In the same way, we get the formula

$$\|f(x) - f_{tria}(x)\| \leq \|f(x) - f_{multi}(x)\| + \varepsilon V$$

Hence

$$\left| \|f(x) - f_{tria}(x)\| - \|f(x) - f_{multi}(x)\| \right| \leq \varepsilon V$$

This means that we can control the accuracy of the approximation through the use of a suitable threshold when some terms are omitted.

Thus, if $f(x)$ is almost a linear function on $[0, L]$, then most of the coefficients $\{\tau_{j,i}\}$ for the current basis functions will be zero.

3.2 Transverse Electric (TE) Case:

Incident field:

$$E_x^i = E_0^i \sin \varphi^i e^{jk_0(x \cos \varphi^i + y \sin \varphi^i)}$$

$$H_z^i = \frac{E_0^i}{\eta_0} e^{jk_0(x \cos \varphi^i + y \sin \varphi^i)}$$

The induced electric current on either side of the surface S_0 can be written in the following form

$$\vec{J}_0^\pm(\vec{r}) = \hat{x} J_0^\pm(x)$$

$$J_0^\pm(x) = \sum_{i=0}^N \tau_{0,i}^\pm \phi_{0,i}(x) + \sum_{v=1}^V \sum_{i=1}^{2^{v-1}N} \tau_{v,i}^\pm \phi_{v,i}(x) \quad (11)$$

The induced electric and magnetic currents on the surface S_1 can be written in the following form

$$\vec{J}_1(\vec{r}) = \hat{x} J_1(x)$$

$$J_1(x) = \sum_{i=0}^N \tau_{0,i}^1 \phi_{0,i}(x) + \sum_{v=1}^V \sum_{i=1}^{2^{v-1}N} \tau_{v,i}^1 \phi_{v,i}(x) \quad (12)$$

$$\vec{M}_1(\vec{r}) = -\hat{z} \eta_0 M_1(x)$$

$$M_1(x) = \sum_{i=0}^N \tau_{0,i}^2 \phi_{0,i}(x) + \sum_{v=1}^V \sum_{i=1}^{2^{v-1}N} \tau_{v,i}^2 \phi_{v,i}(x) \quad (13)$$

On S_1 , we have the following formula:

$$\begin{aligned}
 E_x^i(x, d) = & \frac{\omega\mu_1}{4} \left\{ \int_0^L J_1(x') H_0^{(2)}(k_1|x-x'|) dx' \right. \\
 & \left. + \frac{1}{k_1^2} \frac{\partial}{\partial x} \int_0^L \frac{\partial J_1(x')}{\partial x'} H_0^{(2)}(k_1|x-x'|) dx' \right\} \\
 & + \frac{\omega\mu_2}{4} \left\{ \int_0^L J_1(x') H_0^{(2)}(k_1|x-x'|) dx' \right. \\
 & \left. + \frac{1}{k_2^2} \frac{\partial}{\partial x} \int_0^L \frac{\partial J_1(x')}{\partial x'} H_0^{(2)}(k_2|x-x'|) dx' \right\} \\
 & + \frac{\omega\mu_1}{4} \left\{ \int_0^L J_0^-(x') H_0^{(2)}(k_1 t) dx' \right. \\
 & \left. + \frac{1}{k_1^2} \frac{\partial}{\partial x} \int_0^L \frac{\partial J_0^-(x')}{\partial x'} H_0^{(2)}(k_1 t) dx' \right\} \\
 & - \frac{\omega\mu_2}{4} \left\{ \int_0^L J_0^+(x') H_0^{(2)}(k_2 t) dx' \right. \\
 & \left. + \frac{1}{k_2^2} \frac{\partial}{\partial x} \int_0^L \frac{\partial J_0^+(x')}{\partial x'} H_0^{(2)}(k_2 t) dx' \right\}
 \end{aligned}$$

$$\begin{aligned}
 H_z^i(x, h) = & \frac{-\eta_0\omega\mu_1}{4\eta_1^2} \left\{ \int_0^L M_1(x') H_0^{(2)}(k_1|x-x'|) dx' \right\} \\
 & + \frac{-\eta_0\omega\mu_2}{4\eta_2^2} \left\{ \int_0^L M_1(x') H_0^{(2)}(k_2|x-x'|) dx' \right\} \\
 & + \frac{d}{4j} \left\{ \int_0^L J_0^-(x') \frac{1}{\sqrt{(x-x')^2 + d^2}} \frac{dH_0^{(2)}(k_1 t)}{dt} dx' \right\} \\
 & - \frac{d}{4j} \left\{ \int_0^L J_0^+(x') \frac{1}{\sqrt{(x-x')^2 + d^2}} \frac{dH_0^{(2)}(k_2 t)}{dt} dx' \right\}
 \end{aligned}$$

with

$$t = \sqrt{(x-x')^2 + d^2}$$

On S_0 we have the following formula:

$$\begin{aligned}
E_x^i(x, 0) &= \frac{\omega\mu_1}{4} \left\{ \int_0^L J_1(x') H_0^{(2)}(k_1 t) dx' \right. \\
&\quad \left. + \frac{1}{k_1^2} \frac{\partial}{\partial x} \int_0^L \frac{\partial J_0^-(x')}{\partial x'} H_0^{(2)}(k_1 t) dx' \right\} \\
&\quad + \frac{\eta_0 d}{4j} \left\{ \int_0^L M_1(x') \frac{1}{\sqrt{(x-x')^2 + d^2}} \frac{dH_0^{(2)}(k_1 t)}{dt} dx' \right\} \\
&\quad + \frac{\omega\mu_1}{4} \left\{ \int_0^L J_0^-(x') H_0^{(2)}(k_1 |x-x'|) dx' \right. \\
&\quad \left. + \frac{1}{k_1^2} \frac{\partial}{\partial x} \int_0^L \frac{\partial J_0^-(x')}{\partial x'} H_0^{(2)}(k_1 |x-x'|) dx' \right\} \\
0 &= -\frac{\omega\mu_2}{4} \left\{ \int_0^L J_1(x') H_0^{(2)}(k_2 t) dx' \right. \\
&\quad \left. + \frac{1}{k_2^2} \frac{\partial}{\partial x} \int_0^L \frac{\partial J_1(x')}{\partial x'} H_0^{(2)}(k_2 t) dx' \right\} \\
&\quad + \frac{-\eta_0 d}{4j} \left\{ \int_0^L M_1(x') \frac{1}{\sqrt{(x-x')^2 + d^2}} \frac{dH_0^{(2)}(k_2 t)}{dt} dx' \right\} \\
&\quad + \frac{\omega\mu_2}{4} \left\{ \int_0^L J_0^+(x') H_0^{(2)}(k_1 |x-x'|) dx' \right. \\
&\quad \left. + \frac{1}{k_2^2} \frac{\partial}{\partial x} \int_0^L \frac{\partial J_0^+(x')}{\partial x'} H_0^{(2)}(k_2 |x-x'|) dx' \right\}
\end{aligned}$$

By use of the moment method on the multiscale basis, we obtain the following formula:

$$\begin{aligned}
\langle E_x^i(x, d), \phi_{v', i'}(x) \rangle &= \sum_{v=0}^V \sum_{i=B(v)}^{A(v, N)} \tau_{v, i}^1 \langle L_1^1[\phi_{v, i}(x')] \\
&\quad + L_2^1[\phi_{v, i}(x')], \phi_{v', i'}(x) \rangle \\
&\quad + \sum_{v=0}^V \sum_{i=B(v)}^{A(v, N)} \tau_{v, i}^{0-} \langle L_1^2[\phi_{v, i}(x')], \phi_{v', i'}(x) \rangle \\
&\quad - \sum_{v=0}^V \sum_{i=B(v)}^{A(v, N)} \tau_{v, i}^{0+} \langle L_2^2[\phi_{v, i}(x')], \phi_{v', i'}(x) \rangle
\end{aligned} \tag{14a}$$

$$\begin{aligned}
\langle H_z^i(x, d), \phi_{v', i'}(x) \rangle &= - \sum_{v=0}^V \sum_{i=B(v)}^{A(v, N)} \tau_{v, i}^2 \langle \frac{\eta_0}{\eta_1^2} M_1^1[\phi_{v, i}(x')] \rangle \\
&\quad + \frac{\eta_0}{\eta_2^2} M_2^1[\phi_{v, i}(x')], \phi_{v', i'}(x) \rangle \\
&\quad + d \sum_{v=0}^V \sum_{i=B(v)}^{A(v, N)} \tau_{v, i}^{0-} \langle K_1^2[\phi_{v, i}(x')], \phi_{v', i'}(x) \rangle \\
&\quad - d \sum_{v=0}^V \sum_{i=B(v)}^{A(v, N)} \tau_{v, i}^{0+} \langle K_2^2[\phi_{v, i}(x')], \phi_{v', i'}(x) \rangle
\end{aligned} \tag{14b}$$

$$\begin{aligned}
\langle E_x^i(x, 0), \phi_{v', i'}(x) \rangle &= \sum_{v=0}^V \sum_{i=B(v)}^{A(v, N)} \tau_{v, i}^1 \langle L_1^2[\phi_{v, i}(x')], \phi_{v', i'}(x) \rangle \\
&\quad + d\eta_0 \sum_{v=0}^V \sum_{i=B(v)}^{A(v, N)} \tau_{v, i}^2 \langle K_1^2[\phi_{v, i}(x')], \phi_{v', i'}(x) \rangle \tag{14c} \\
&\quad + \sum_{v=0}^V \sum_{i=B(v)}^{A(v, N)} \tau_{v, i}^{0-} \langle L_1^1[\phi_{v, i}(x')], \phi_{v', i'}(x) \rangle
\end{aligned}$$

$$\begin{aligned}
0 &= - \sum_{v=0}^V \sum_{i=B(v)}^{A(v, N)} \tau_{v, i}^1 \langle L_2^2[\phi_{v, i}(x')], \phi_{v', i'}(x) \rangle \\
&\quad - d\eta_0 \sum_{v=0}^V \sum_{i=B(v)}^{A(v, N)} \tau_{v, i}^2 \langle K_2^2[\phi_{v, i}(x')], \phi_{v', i'}(x) \rangle \tag{14d} \\
&\quad + \sum_{v=0}^V \sum_{i=B(v)}^{A(v, N)} \tau_{v, i}^{0+} \langle L_2^1[\phi_{v, i}(x')], \phi_{v', i'}(x) \rangle
\end{aligned}$$

where

$$\begin{aligned}
v' &= 0, 1, 2, \dots, V, i' = B(v'), \dots, A(v', N) \\
A(v, N) &= \begin{cases} N+1 & v=0 \\ 2^{v-1}N & v \neq 0 \end{cases} \quad B(v) = \begin{cases} 0 & v=0 \\ 1 & v \neq 0 \end{cases}
\end{aligned}$$

$$\begin{aligned}
L_i^1[X(x')] &= \frac{\omega\mu_i}{4} \left\{ \int_0^L X(x') H_0^{(2)}(k_i|x-x'|) dx' \right. \\
&\quad \left. + \frac{1}{k_i^2} \frac{\partial}{\partial x} \int_0^L \frac{\partial X(x')}{\partial x'} H_0^{(2)}(k_i|x-x'|) dx' \right\} \\
L_i^2[X(x')] &= \frac{\omega\mu_i}{4} \left\{ \int_0^L X(x') H_0^{(2)}(k_i t) dx' \right. \\
&\quad \left. + \frac{1}{k_i^2} \frac{\partial}{\partial x} \int_0^L \frac{\partial X(x')}{\partial x'} H_0^{(2)}(k_i t) dx' \right\} \\
&\quad \text{with } t = \sqrt{(x-x')^2 + d^2} \\
M_i^1[X(x')] &= \frac{\omega\mu_i}{4} \left\{ \int_0^L X(x') H_0^{(2)}(k_i|x-x'|) dx' \right\} \\
M_i^2[X(x')] &= \frac{\omega\mu_i}{4} \left\{ \int_0^L X(x') H_0^{(2)}(k_i \sqrt{(x-x')^2 + d^2}) dx' \right\} \\
K_i^1[X(x')] &= \frac{1}{4j} \left\{ \int_0^L \frac{X(x')}{|x-x'|} \frac{dH_0^{(2)}(k_i|x-x'|)}{dt} dx' \right\} \\
&= \frac{-k_i}{4j} \left\{ \int_0^L X(x') \frac{H_1^{(2)}(k_i|x-x'|)}{|x-x'|} dx' \right\} \\
K_i^2[X(x')] &= \frac{1}{4j} \left\{ \int_0^L \frac{X(x')}{\sqrt{(x-x')^2 + d^2}} \right. \\
&\quad \left. \frac{dH_0^{(2)}(k_i \sqrt{(x-x')^2 + d^2})}{dt} dx' \right\} \\
&= \frac{-k_i}{4j} \left\{ \int_0^L X(x') \frac{H_1^{(2)}(k_i \sqrt{(x-x')^2 + d^2})}{\sqrt{(x-x')^2 + d^2}} dx' \right\}
\end{aligned}$$

Once the above equations are solved, the bistatic radar cross section can be computed by

$$\begin{aligned}
\sigma(\varphi, \varphi^i) &= \lim_{r \rightarrow \infty} 2\pi r \frac{|\vec{H}^s|^2}{|\vec{H}^i|^2} \\
&= \frac{k_1 \eta_0^2}{4} \left| \xi_{0,0} \frac{1}{jk_1 \cos \varphi} \left[e^{\frac{jk_1 h \cos \varphi}{2}} \text{SINC} \left(\frac{k_1 h \cos \varphi}{2} \right) - 1 \right] \right. \\
&\quad \left. + \xi_{0,N} \frac{e^{jk_1 L \cos \varphi}}{jk_1 \cos \varphi} \left[1 - e^{-\frac{jk_1 h \cos \varphi}{2}} \text{SINC} \left(\frac{k_1 h \cos \varphi}{2} \right) \right] \right|
\end{aligned}$$

$$\begin{aligned}
& + \sum_{i=1}^{N-1} \xi_{0,i} e^{jk_1 x_{0,i} \cos \varphi} h \text{SINC}^2 \left(\frac{k_1 h \cos \varphi}{2} \right) + \\
& \sum_{v=1}^V \sum_{i=1}^{2^{v-1}N} \xi_{v,i} e^{jk_1 x_{v,i} \cos \varphi} \frac{h}{2^v} \text{SINC}^2 \left(\frac{k_1 h \cos \varphi}{2^{v+1}} \right) \Big|^2
\end{aligned}$$

where

$$\xi_{v,i} = \sin \varphi (\tau_{v,i}^1 e^{jk_1 d \sin \varphi} + \tau_{v,i}^{0-}) + \frac{\eta_0}{\eta_1} e^{jk_1 d \sin \varphi} \tau_{v,i}^2$$

where the *SINC* function is defined by $\sin x/x$. And the scattered magnetic field is given as

$$\begin{aligned}
\vec{H}^s(\vec{r}) = & \sqrt{\frac{k_1}{8\pi}} e^{\frac{j\pi}{4}} \frac{e^{-jk_1 r}}{\sqrt{r}} \int_0^L \left[\sin \varphi (J_1(x') e^{jk_1 d \sin \varphi} + J_0^-(x')) \right. \\
& \left. + \frac{\eta_0}{\eta_1} e^{jk_1 d \sin \varphi} M_1(x') \right] e^{jk_1 x' \cos \varphi} dx' \hat{z}
\end{aligned}$$

3.3 Transverse Magnetic (TM) case:

Incident field:

$$\begin{aligned}
E_z^i &= E_0^i e^{jk_0(x \cos \varphi^i + y \sin \varphi^i)} \\
H_x^i &= -\frac{E_0^i}{\eta_0} \sin \varphi^i e^{jk_0(x \cos \varphi^i + y \sin \varphi^i)}
\end{aligned}$$

The induced electric current on either side of the surface S_0 can be written in the following form

$$\begin{aligned}
\vec{J}_0^\pm(\vec{r}) &= -\hat{z} J_0^\pm(x) \\
J_0^\pm(x) &= \sum_{i=0}^N \tau_{0,i}^\pm \phi_{0,i}(x) + \sum_{v=1}^V \sum_{i=1}^{2^{v-1}N} \tau_{v,i}^\pm \phi_{v,i}(x)
\end{aligned} \tag{15}$$

The induced electric and magnetic currents on the surface S_1 can be written in the following form

$$\begin{aligned}
\vec{J}_1(\vec{r}) &= -\hat{z} J_1(x) \\
J_1(x) &= \sum_{i=0}^N \tau_{0,i}^1 \phi_{0,i}(x) + \sum_{v=1}^V \sum_{i=1}^{2^{v-1}N} \tau_{v,i}^1 \phi_{v,i}(x)
\end{aligned} \tag{16}$$

$$\begin{aligned}\vec{M}_1(\vec{r}) &= \hat{x}\eta_0 M_1(x) \\ M_1(x) &= \sum_{i=0}^N \tau_{0,i}^2 \phi_{0,i}(x) + \sum_{v=1}^V \sum_{i=1}^{2^{v-1}N} \tau_{v,i}^2 \phi_{v,i}(x)\end{aligned}\quad (17)$$

On S_1 , we have the following formula:

$$\begin{aligned}E_z^i(x, h) &= -\frac{\omega\mu_1}{4} \left\{ \int_0^L J_1(x') H_0^{(2)}(k_1|x-x'|) dx' \right\} \\ &\quad - \frac{\omega\mu_2}{4} \left\{ \int_0^L J_1(x') H_0^{(2)}(k_2|x-x'|) dx' \right\} \\ &\quad - \frac{\omega\mu_1}{4} \left\{ \int_0^L J_0^-(x') H_0^{(2)}(k_1 t) dx' \right\} \\ &\quad + \frac{\omega\mu_2}{4} \left\{ \int_0^L J_0^+(x') H_0^{(2)}(k_2 t) dx' \right\} \\ H_z^i(x, h) &= \frac{\eta_0\omega\mu_1}{4\eta_1^2} \left\{ \int_0^L M_1(x') H_0^{(2)}(k_1|x-x'|) dx' \right. \\ &\quad \left. + \frac{1}{k_1^2} \frac{\partial}{\partial x} \int_0^L \frac{\partial M_1(x')}{\partial x'} H_0^{(2)}(k_1|x-x'|) dx' \right\} \\ &\quad + \frac{\eta_0\omega\mu_2}{4\eta_2^2} \left\{ \int_0^L M_1(x') H_0^{(2)}(k_2|x-x'|) dx' \right. \\ &\quad \left. + \frac{1}{k_2^2} \frac{\partial}{\partial x} \int_0^L \frac{\partial M_1(x')}{\partial x'} H_0^{(2)}(k_2|x-x'|) dx' \right\} \\ &\quad + \frac{d}{4j} \left\{ \int_0^L J_0^-(x') \frac{1}{\sqrt{(x-x')^2 + d^2}} \frac{dH_0^{(2)}(k_1 t)}{dt} dx' \right\} \\ &\quad - \frac{d}{4j} \left\{ \int_0^L J_0^+(x') \frac{1}{\sqrt{(x-x')^2 + d^2}} \frac{dH_0^{(2)}(k_2 t)}{dt} dx' \right\}\end{aligned}$$

On S_0 , we have the following formula:

$$\begin{aligned}E_x^i(x, 0) &= \frac{\omega\mu_1}{-4} \left\{ \int_0^L J_1(x') H_0^{(2)}(k_1 t) dx' \right\} \\ &\quad + \frac{\eta_0 d}{4j} \left\{ \int_0^L M_1(x') \frac{1}{\sqrt{(x-x')^2 + d^2}} \frac{dH_0^{(2)}(k_1 t)}{dt} dx' \right\} \\ &\quad + \frac{\omega\mu_1}{-4} \left\{ \int_0^L J_0^-(x') H_0^{(2)}(k_1|x-x'|) dx' \right\}\end{aligned}$$

$$\begin{aligned}
0 = & \frac{\omega\mu_2}{4} \left\{ \int_0^L J_1(x') H_0^{(2)}(k_2 t) dx' \right\} \\
& + \frac{\eta_0 d}{-4j} \left\{ \int_0^L M_1(x') \frac{1}{\sqrt{(x-x')^2 + d^2}} \frac{dH_0^{(2)}(k_2 t)}{dt} dx' \right\} \\
& + \frac{\omega\mu_2}{-4} \left\{ \int_0^L J_0^+(x') H_0^{(2)}(k_1 |x-x'|) dx' \right\}
\end{aligned}$$

By use of moment method on the multiscale basis, we obtain the following formula:

$$\begin{aligned}
\langle E_x^i(x, h), \phi_{v', i'}(x) \rangle = & - \sum_{v=0}^V \sum_{i=B(v)}^{A(v, N)} \tau_{v, i}^1 \langle M_1^1[\phi_{v, i}(x')] \\
& + M_2^1[\phi_{v, i}(x')], \phi_{v', i'}(x) \rangle \\
& - \sum_{v=0}^V \sum_{i=B(v)}^{A(v, N)} \tau_{v, i}^{0-} \langle M_1^2[\phi_{v, i}(x')], \phi_{v', i'}(x) \rangle \quad (18a)
\end{aligned}$$

$$\begin{aligned}
& + \sum_{v=0}^V \sum_{i=B(v)}^{A(v, N)} \tau_{v, i}^{0+} \langle M_2^2[\phi_{v, i}(x')], \phi_{v', i'}(x) \rangle \\
\langle H_z^i(x, h), \phi_{v', i'}(x) \rangle = & \sum_{v=0}^V \sum_{i=B(v)}^{A(v, N)} \tau_{v, i}^2 \langle \frac{\eta_0}{\eta_1^2} L_1^1[\phi_{v, i}(x')] \\
& + \frac{\eta_0}{\eta_2^2} L_2^1[\phi_{v, i}(x')], \phi_{v', i'}(x) \rangle \quad (18b) \\
& + d \sum_{v=0}^V \sum_{i=B(v)}^{A(v, N)} \tau_{v, i}^{0-} \langle K_1^2[\phi_{v, i}(x')], \phi_{v', i'}(x) \rangle \\
& - d \sum_{v=0}^V \sum_{i=B(v)}^{A(v, N)} \tau_{v, i}^{0+} \langle K_2^2[\phi_{v, i}(x')], \phi_{v', i'}(x) \rangle
\end{aligned}$$

$$\begin{aligned}
\langle E_x^i(x, 0), \phi_{v', i'}(x) \rangle = & - \sum_{v=0}^V \sum_{i=B(v)}^{A(v, N)} \tau_{v, i}^1 \langle M_1^2[\phi_{v, i}(x')], \phi_{v', i'}(x) \rangle \\
& + d\eta_0 \sum_{v=0}^V \sum_{i=B(v)}^{A(v, N)} \tau_{v, i}^2 \langle K_1^2[\phi_{v, i}(x')], \phi_{v', i'}(x) \rangle \quad (18c) \\
& - \sum_{v=0}^V \sum_{i=B(v)}^{A(v, N)} \tau_{v, i}^{0-} \langle M_1^1[\phi_{v, i}(x')], \phi_{v', i'}(x) \rangle
\end{aligned}$$

$$\begin{aligned}
0 = & \sum_{v=0}^V \sum_{i=B(v)}^{A(v, N)} \tau_{v, i}^1 \langle M_2^2[\phi_{v, i}(x')], \phi_{v', i'}(x) \rangle \\
& - d\eta_0 \sum_{v=0}^V \sum_{i=B(v)}^{A(v, N)} \tau_{v, i}^2 \langle K_2^2[\phi_{v, i}(x')], \phi_{v', i'}(x) \rangle \quad (18d) \\
& - \sum_{v=0}^V \sum_{i=B(v)}^{A(v, N)} \tau_{v, i}^{0+} \langle L_2^1[\phi_{v, i}(x')], \phi_{v', i'}(x) \rangle
\end{aligned}$$

$$\begin{aligned}
L_i^1[X(x')] = & \frac{\omega\mu_i}{4} \left\{ \int_0^L X(x') H_0^{(2)}(k_i|x-x'|) dx' \right. \\
& \left. + \frac{1}{k_i^2} \frac{\partial}{\partial x} \int_0^L \frac{\partial X(x')}{\partial x'} H_0^{(2)}(k_i|x-x'|) dx' \right\}
\end{aligned}$$

$$\begin{aligned}
L_i^2[X(x')] = & \frac{\omega\mu_i}{4} \left\{ \int_0^L X(x') H_0^{(2)}(k_i t) dx' \right. \\
& \left. + \frac{1}{k_i^2} \frac{\partial}{\partial x} \int_0^L \frac{\partial X(x')}{\partial x'} H_0^{(2)}(k_i t) dx' \right\}
\end{aligned}$$

$$M_i^1[X(x')] = \frac{\omega\mu_i}{4} \left\{ \int_0^L X(x') H_0^{(2)}(k_i|x-x'|) dx' \right\}$$

$$M_i^2[X(x')] = \frac{\omega\mu_i}{4} \left\{ \int_0^L X(x') H_0^{(2)}(k_i \sqrt{(x-x')^2 + d^2}) dx' \right\}$$

$$K_i^1[X(x')] = \frac{-k_i}{4j} \left\{ \int_0^L X(x') \frac{H_1^{(2)}(k_i|x-x'|)}{|x-x'|} dx' \right\}$$

$$K_i^2[X(x')] = \frac{-k_i}{4j} \left\{ \int_0^L X(x') \frac{H_1^{(2)}(k_i\sqrt{(x-x')^2+d^2})}{\sqrt{(x-x')^2+d^2}} dx' \right\}$$

Once the above equations are solved, the bistatic radar cross section can be computed by

$$\begin{aligned} \sigma(\varphi, \varphi^i) &= \lim_{r \rightarrow \infty} 2\pi r \frac{|\vec{E}^s|^2}{|\vec{E}^i|^2} \\ &= \frac{k_1}{4} \left| \xi_{0,0} \frac{1}{jk_1 \cos \varphi} \left[e^{\frac{jk_1 h \cos \varphi}{2}} \text{SINC} \left(\frac{k_1 h \cos \varphi}{2} \right) - 1 \right] \right. \\ &\quad + \xi_{0,N} \frac{e^{jk_1 L \cos \varphi}}{jk_1 \cos \varphi} \left[1 - e^{-\frac{jk_1 h \cos \varphi}{2}} \text{SINC} \left(\frac{k_1 h \cos \varphi}{2} \right) \right] \\ &\quad + \sum_{i=1}^{N-1} \xi_{0,i} e^{jk_1 x_{0,i} \cos \varphi} h \text{SINC}^2 \left(\frac{k_1 h \cos \varphi}{2} \right) \\ &\quad \left. + \sum_{v=1}^V \sum_{i=1}^{2^{v-1}N} \xi_{v,i} e^{jk_1 x_{v,i} \cos \varphi} \frac{h}{2^v} \text{SINC}^2 \left(\frac{k_1 h \cos \varphi}{2^{v+1}} \right) \right|^2 \end{aligned}$$

where

$$\xi_{v,i} = \eta_1(\tau_{v,i}^1 e^{jk_1 d \sin \varphi} + \tau_{v,i}^{0-}) - \eta_0 e^{jk_1 d \sin \varphi} \tau_{v,i}^2$$

and the scattered electric field is given by

$$\begin{aligned} \vec{E}^s(\vec{r}) &= \sqrt{\frac{k_1}{8\pi}} e^{\frac{j\pi}{4}} \frac{e^{-jk_1 r}}{\sqrt{r}} \int_0^L \left[\eta_1 (J_1(x') e^{jk_1 d \sin \varphi} + J_0^-(x')) \right. \\ &\quad \left. - \eta_0 e^{jk_1 d \sin \varphi} M_1(x') \right] e^{jk_1 x' \cos \varphi} dx' \hat{z} \end{aligned}$$

4. ADAPTIVE ALGORITHM FOR LINEAR EQUATIONS USING THE MULTISCALE BASIS

In this section, we discuss how to solve the linear equations of (14a–14d) or (18–18d) by use of AMMM.

The linear equations of (11a–11d) or (14a–14d) can be written in the following matrix form:

$$\begin{pmatrix} A_{1,1} & A_{1,2} & A_{1,3} & O \\ A_{1,2} & A_{2,2} & O & A_{2,4} \\ A_{1,3} & O & A_{3,3} & A_{3,4} \\ O & A_{2,4} & A_{3,4} & A_{4,4} \end{pmatrix} \begin{pmatrix} J_0^- \\ J_1 \\ M_1 \\ J_0^+ \end{pmatrix} = \begin{pmatrix} F_1 \\ F_2 \\ F_3 \\ O \end{pmatrix} \quad (19)$$

where

$$A_{1,1} = \begin{cases} \langle L_1^1[\phi_{v,i}], \phi_{v',i'} \rangle & \text{for TE case} \\ -\langle M_1^1[\phi_{v,i}], \phi_{v',i'} \rangle & \text{for TM case} \end{cases}$$

$$A_{1,2} = \begin{cases} \langle L_1^2[\phi_{v,i}], \phi_{v',i'} \rangle & \text{for TE case} \\ -\langle M_1^2[\phi_{v,i}], \phi_{v',i'} \rangle & \text{for TM case} \end{cases}$$

$$A_{1,3} = d\eta_0 \langle K_1^2[\phi_{v,i}], \phi_{v',i'} \rangle \quad \text{for TE and TM}$$

$$A_{2,2} = \begin{cases} \langle (L_1^1 + L_2^1)[\phi_{v,i}], \phi_{v',i'} \rangle & \text{for TE case} \\ -\langle (M_1^1 + M_2^1)[\phi_{v,i}], \phi_{v',i'} \rangle & \text{for TM case} \end{cases}$$

$$A_{2,4} = \begin{cases} -\langle L_2^2[\phi_{v,i}], \phi_{v',i'} \rangle & \text{for TE case} \\ \langle M_2^2[\phi_{v,i}], \phi_{v',i'} \rangle & \text{for TM case} \end{cases}$$

$$A_{3,3} = \begin{cases} -\langle \left(\frac{\eta_0^2}{\eta_1^2} M_1^1 + \frac{\eta_0^2}{\eta_2^2} M_2^1 \right) [\phi_{v,i}], \phi_{v',i'} \rangle & \text{for TE case} \\ \langle \left(\frac{\eta_0^2}{\eta_1^2} L_1^1 + \frac{\eta_0^2}{\eta_2^2} L_2^1 \right) [\phi_{v,i}], \phi_{v',i'} \rangle & \text{for TM case} \end{cases}$$

$$A_{3,4} = -d\eta_0 \langle K_2^2[\phi_{v,i}], \phi_{v',i'} \rangle \quad \text{for TE and TM cases}$$

$$A_{4,4} = \begin{cases} \langle L_1^1[\phi_{v,i}], \phi_{v',i'} \rangle & \text{for TE case} \\ -\langle M_2^1[\phi_{v,i}], \phi_{v',i'} \rangle & \text{for TM case} \end{cases}$$

$$F_1 = \begin{cases} \langle \sin \phi^i \exp(jk_0 x \cos \phi^i), \phi_{v',i'} \rangle & \text{for TE case} \\ \langle \exp(jk_0 x \cos \phi^i), \phi_{v',i'} \rangle & \text{for TM case} \end{cases}$$

$$F_2 = \begin{cases} \langle \sin \phi^i \exp(jk_0 x \cos \phi^i + d \sin \phi^i), \phi_{v',i'} \rangle & \text{for TE case} \\ \langle \exp(jk_0 x \cos \phi^i + d \sin \phi^i), \phi_{v',i'} \rangle & \text{for TM case} \end{cases}$$

$$F_3 = \begin{cases} \langle \exp(jk_0 x \cos \phi^i + d \sin \phi^i), \phi_{v',i'} \rangle & \text{for TE case} \\ -\langle \sin \phi^i \exp(jk_0 x \cos \phi^i + d \sin \phi^i), \phi_{v',i'} \rangle & \text{for TM case} \end{cases}$$

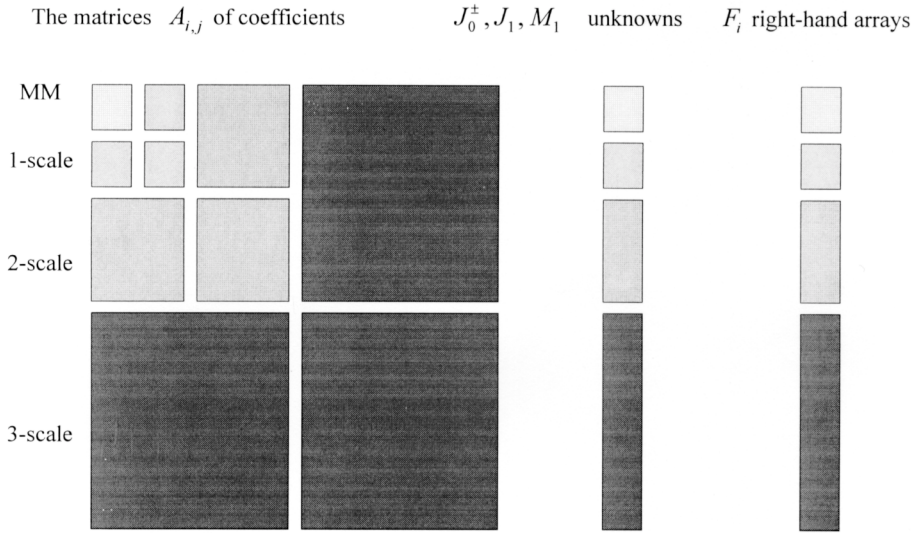


Figure 3. The assembly of the coefficient matrices, right-hand arrays of the known incident field, and the unknowns.

All of elements of the matrix or the array \mathbf{O} are zero.

The illustration of these matrices $A_{i,j}$, the arrays F_i , and the unknowns (J_0^\pm, J_1, M_1) can be arranged on the multiscale (see Fig. 3). When $V = 0$, the linear equation is the same as the equations obtained by standard MOM, which can be solved by LU method or the iterative methods. The first step is to predict the solution on $(V+1)$ -scale from the known solution on V -scale by the interpolation method. Each unknown functions can be denoted simply by $X_{V+1}(x)$. The unknown coefficients J_0^\pm, J_1, M_1 on V -th scale is denoted by $X_v = (\tau_{v,1}, \tau_{v,2}, \dots, \tau_{v,2^{v-1}N})^T$.

Between the unknown approximation function on $(V+1)$ -scale and the known approximation function, there is the following relation:

$$X_{V+1}(x) = X_V(x) + \sum_{i=1}^{2^v N} \tau_{V+1,i} \phi_{V+1,i}(x)$$

Hence, the known solution $X_V(x)$ on V -scale can be chosen as an initial guess for the unknown solution $X_{V+1}(x)$ on $(V+1)$ -scale if $\{\tau_{V+1,i}\}$ are set to be zero. However, $\tau_{V+1,i}$ can be estimated from

$X_V(x)$ by the interpolation method, noted as $X_{V+1}^{(0)} = (\tau_{V+1,1}^{(0)}, \tau_{V+1,2}^{(0)}, \dots, \tau_{V+1,2^V N}^{(0)})^T$. Therefore, the initial array $(X_0, X_1, \dots, X_V, X_{V+1})$ can be constructed from the known array (X_0, X_1, \dots, X_V) by the solution of the function $X_V(x)$ and the array $X_{V+1}^{(0)}$ can be estimated from $X_V(x)$.

The second step is to eliminate the relatively smaller components of the predicted solution components and omit the corresponding rows and columns from the system matrix obtained from the moment method.

If $|\tau_{v,i}^{(0)}| \leq \varepsilon$ ($v = 1, 2, \dots, V+1, i = 1, 2, \dots, 2^V N$, ε is threshold), we set $\tau_{v,i}^{(0)} = 0$, and omit the corresponding arrays and columns of the system matrix with respect to (v, i) . This is an important step to reduce the size of the linear equation.

In actual computation, we choose the following criterion $|\tau_{v,i}^{(0)}| \leq \varepsilon T$ ($T = \max |\tau_{v,i}^{(0)}|$).

The third step is to solve the modified linear equation after the above two steps by use of the CG method or other iterative methods.

The final step is to obtain the solution $X_{V+1}(x)$ on the $(V+1)$ -scale by adding some of the terms, whose coefficients are zero.

Because the order of the original linear equation is reduced, it will improve the computational efficiency. The flow chart for the adaptive multiscale moment method from V -time scale to $(V+1)$ -time scale is given in Fig. 4.

5. NUMERICAL RESULTS

Numerical calculations were performed by use of the procedure described in the above section to demonstrate the effectiveness of the adaptive multiscale moment method.

The first example was a 1λ "free-space" coated strip with 0.01λ thickness with a TM illumination. The orders of the linear equation of AMMM for different threshold and incident angles are listed in Tables (I) and (II). The number of the initial division N is taken as 8.

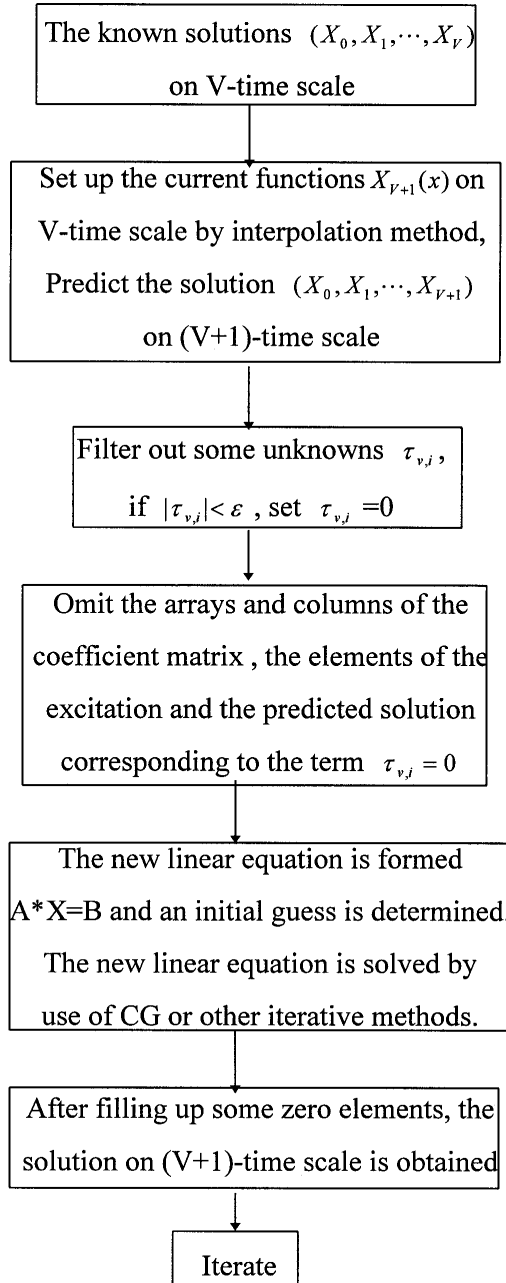


Figure 4. Flow chart of the adaptive multiscale moment method.

TABLE (I). Normal incidence

N=8	$\varepsilon=0.$					$\varepsilon=0.01$					$\varepsilon=0.1$				
	J_0^+	J_0^-	J_1	M_1	Σ	J_0^+	J_0^-	J_1	M_1	Σ	J_0^+	J_0^-	J_1	M_1	Σ
V=0	9	9	9	7	34	9	9	9	7	34	9	9	9	7	34
V=1	17	17	17	15	66	17	16	15	15	63	9	13	9	15	46
V=2	33	33	33	31	130	20	20	18	27	85	9	15	9	25	58
V=3	65	65	65	63	258	26	21	23	43	113	9	17	9	43	78
V=4	129	129	129	127	514	45	24	29	77	175	9	19	9	77	114
V=5	257	257	257	255	1026	91	32	50	145	318	9	17	9	140	175

where Σ means the number of total unknowns.

TABLE (II). Incident angle $\phi = 45^\circ$

N=8	$\varepsilon=0.$					$\varepsilon=0.01$					$\varepsilon=0.1$				
	J_0^+	J_0^-	J_1	M_1	Σ	J_0^+	J_0^-	J_1	M_1	Σ	J_0^+	J_0^-	J_1	M_1	Σ
V=0	9	9	9	7	34	9	9	9	7	34	9	9	9	7	34
V=1	17	17	17	15	66	16	17	17	15	65	15	12	14	14	55
V=2	33	33	33	31	130	32	19	32	31	114	22	13	15	20	70
V=3	65	65	65	63	258	56	19	47	50	172	31	14	12	32	89
V=4	129	129	129	127	514	108	20	75	83	286	41	14	12	52	119
V=5	257	257	257	255	1026	221	23	168	149	561	55	13	14	91	173

TABLE (III). Normal incidence: TE case

N=8	$\varepsilon=0.$					$\varepsilon=0.01$					$\varepsilon=0.1$				
	J_0^+	J_0^-	J_1	M_1	Σ	J_0^+	J_0^-	J_1	M_1	Σ	J_0^+	J_0^-	J_1	M_1	Σ
V=0	7	7	7	9	30	7	7	7	9	30	7	7	7	9	30
V=1	15	15	15	17	64	15	15	15	17	62	11	14	11	13	49
V=2	31	31	31	33	126	31	31	31	31	124	15	23	15	16	69
V=3	63	63	63	65	254	63	63	63	27	216	20	40	21	16	97
V=4	127	127	127	129	510	119	127	121	26	393	20	48	20	18	106
V=5	255	255	255	257	1022	170	234	171	28	603	19	44	19	20	102

It is seen from Tables (I) and (II) that the size of the moment matrix can be significantly reduced by utilizing different scales V and setting different thresholds ε to set the unknowns equal to zero by setting $(\tau_{v,i}^{0\pm}, \tau_{v,i}^1, \tau_{v,i}^2)$. The case $\varepsilon = 0$ would be the standard MOM. For TM case, the unknowns for the electric currents J_0^\pm, J_1 , can be reduced

much more than the unknowns for magnetic current M_1 because the variation of the electric currents on the interval $[0, L]$ which are infinite at the ends is relatively smaller than that of the magnetic current on the same interval which is zero at the ends. For TE case, the unknowns for magnetic currents M_1 can be reduced much more than the unknowns for the electric current J_0^\pm, J_1 because the variation of the magnetic current on the interval $[0, L]$ is infinite at the ends and is relatively smaller than that of electric currents on the same interval which are zero at the ends. The magnitude and the phase of the equivalent electric and magnetic currents (J_0^\pm, J_1, M_1) for the TE case of the incident angle $\phi = 45^\circ$ and $\varepsilon = 0.01$ are plotted in Fig. 5.

The second example is a 5.221λ “free-space” coated strip with 0.01λ thickness. The orders of the linear equation for AMMM for different threshold with normal incidence are listed in Tables (III) and (IV) for TE and TM cases, respectively. The number of the initial division N is taken as 8.

It is seen from Tables (III) and (IV) that the size of the moment matrix can be significantly reduced by utilizing different scales V and setting different thresholds ε to set the coefficients $(\tau_{v,i}^{0\pm}, \tau_{v,i}^1, \tau_{v,i}^2)$ to zero from the unknowns at $(V + 1)$ -scale .

TABLE (IV). Normal incidence: TM case

N=8	$\varepsilon=0.$					$\varepsilon=0.01$					$\varepsilon=0.1$				
	J_0^+	J_0^-	J_1	M_1	Σ	J_0^+	J_0^-	J_1	M_1	Σ	J_0^+	J_0^-	J_1	M_1	Σ
V=0	9	9	9	7	34	9	9	9	7	34	7	7	7	9	34
V=1	17	17	17	15	66	15	16	15	15	61	11	13	11	14	49
V=2	33	33	33	31	130	19	23	20	30	92	14	17	13	29	73
V=3	65	65	65	63	258	25	25	25	58	133	13	17	13	45	88
V=4	129	129	129	127	514	30	24	29	93	176	13	19	13	76	121
V=5	257	257	257	255	1026	33	28	34	184	279	13	21	13	143	190

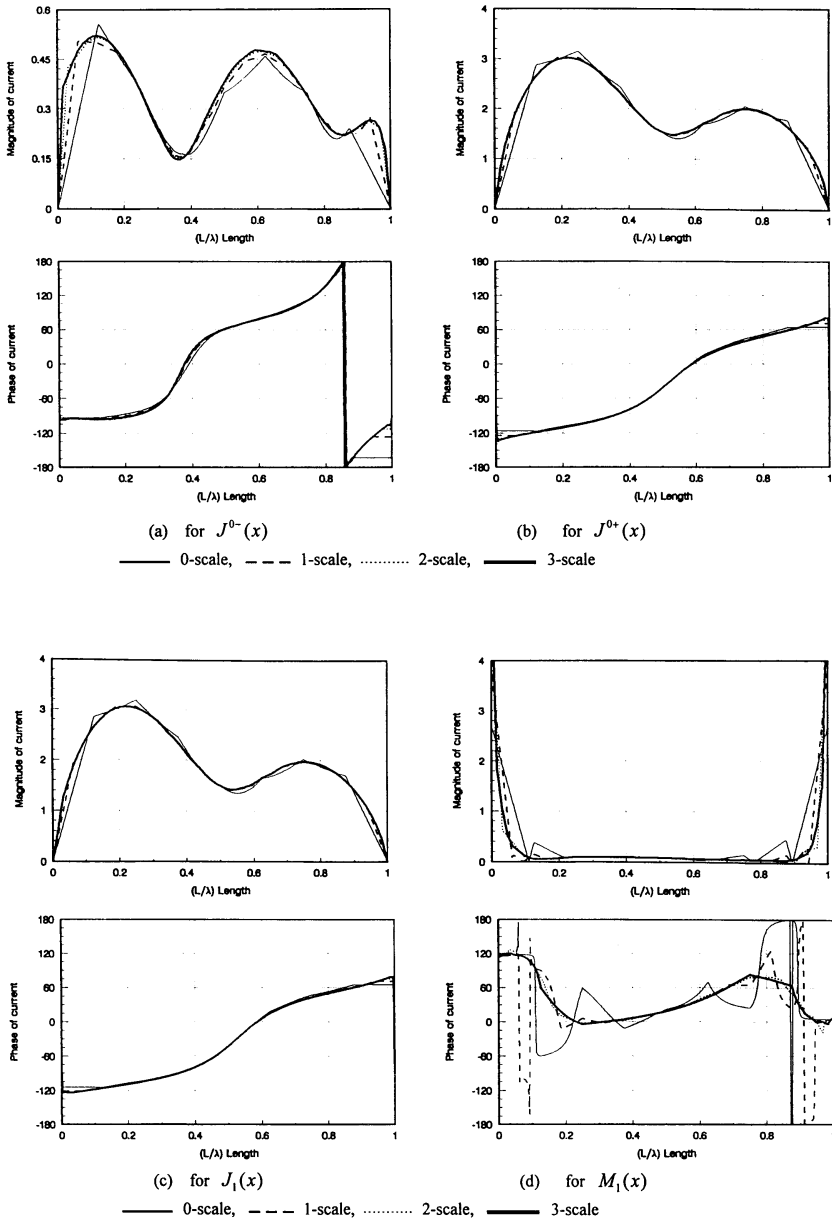


Figure 5(a-d) The magnitude and phase of the equivalent electric and magnetic currents

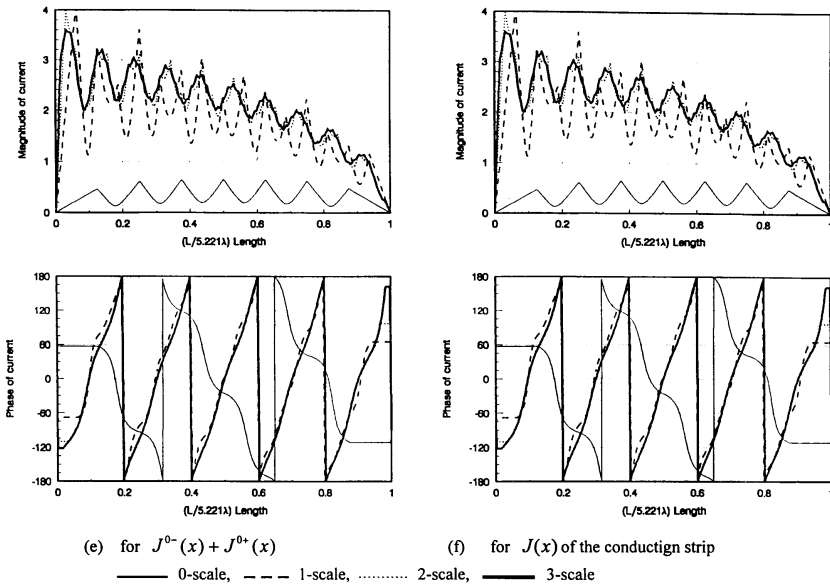


Figure 5(e)(f). The magnitude and phase of the equivalent electric currents.

The magnitudes and the phases of the equivalent currents (J_0^\pm , J_1 , M_1) for the case of the incident angle $\phi = 22^\circ$ and $\varepsilon = 0.01$ are plotted in Fig. 6. These results closely correlate with the results of reference [2]. The curves for the monostatic RCS for TE and TM cases are plotted in Fig. 7 and Fig. 8. For TE polarization, the backscattered field at $\theta = 0$ vanishes for perfectly conducting strip because the edge of the strip is cross polarized to the incident electric field. The backscattered radar cross section including only upper equivalent electric current J_0^+ and lower equivalent electric current J_0^- is in good agreement with RCS of the perfectly conducting strip for the same width (see Fig. 9). For TM case, the results are generally in good agreement with the perfectly conducting case.

The effect of reduced numbers of the unknowns (J_0^\pm, J_1, M_1) through the threshold $\varepsilon = 0.01$ for TM case for different incident angles are plotted in Fig. 10.

The third example is a 8.23λ coated strip with a dielectric coatings ($\varepsilon_{2r} = 2$.) of 0.057λ thickness for the TM case. The orders of the linear equation of AMMM for different thresholds of normal incidence are listed in Table V. The number of the initial division N is taken as 8.

TABLE (V). Normal incidence.

N=8	$\varepsilon=0.$					$\varepsilon=0.01$					$\varepsilon=0.1$				
	J_0^+	J_0^-	J_1	M_1	Σ	J_0^+	J_0^-	J_1	M_1	Σ	J_0^+	J_0^-	J_1	M_1	Σ
V=0	9	9	9	7	34	9	9	9	7	34	9	9	9	7	34
V=1	17	17	17	15	66	15	15	15	15	60	11	13	11	14	49
V=2	33	33	33	31	130	21	26	21	31	99	15	17	13	27	72
V=3	65	65	65	63	258	28	23	29	53	133	15	17	13	43	88
V=4	129	129	129	127	514	34	26	32	89	181	15	19	13	77	124
V=5	257	257	257	255	1026	40	31	33	155	259	15	21	11	143	190

It is seen from Table (V) that the size of the moment matrix for 8.23λ coating strip with dielectric coatings for the TM case can also be significantly reduced by utilizing different scales V and setting different thresholds ε for the unknowns equal to zero through $(\tau_{v,i}^{0\pm}, \tau_{v,i}^1, \tau_{v,i}^2)$.

Monostatic RCS for TE case is plotted in Fig. 11. The computational results are very close to the experiment results [2] for all angles. The number of unknowns (J_0^\pm, J_1, M_1) for the TE case are different from the different incident angles.

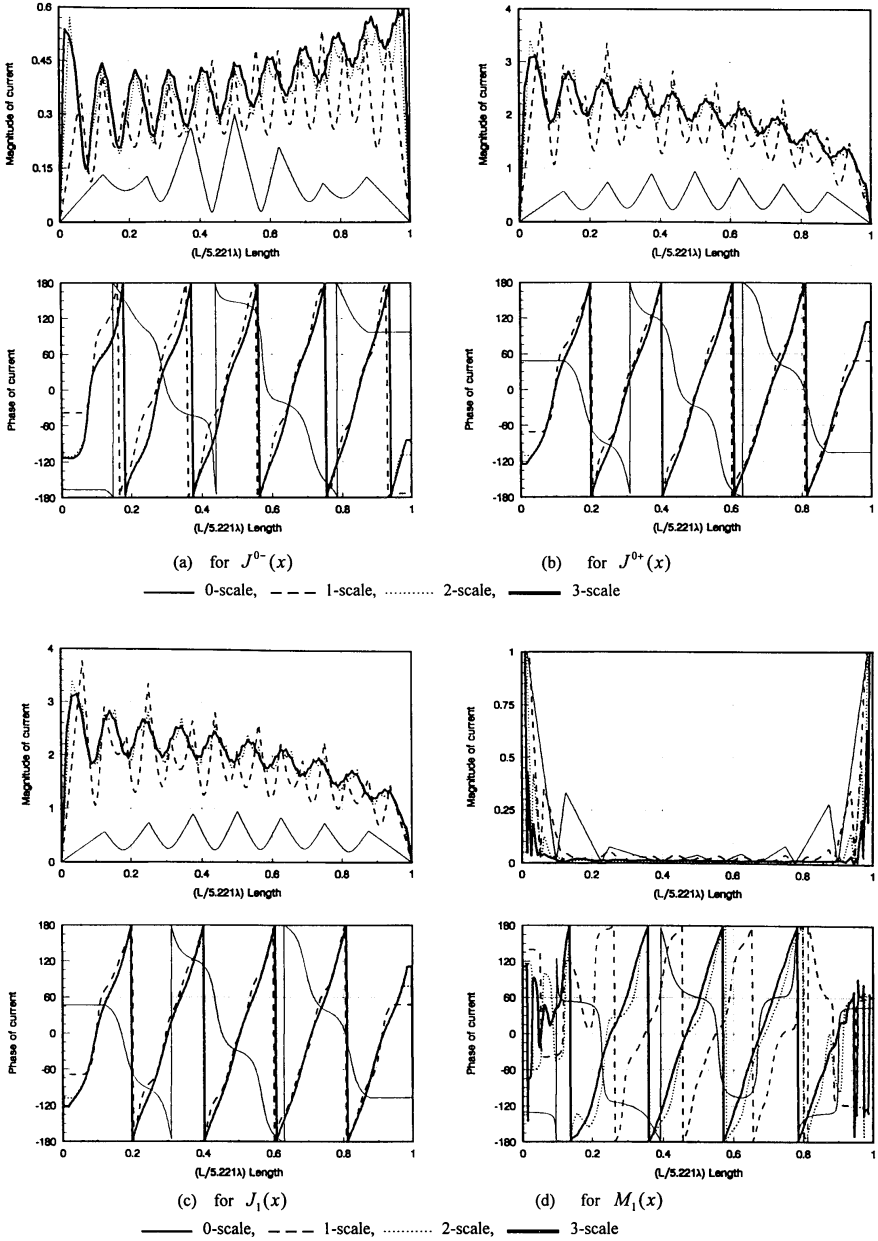


Figure 6. The magnitude and phase of the equivalent electric currents.

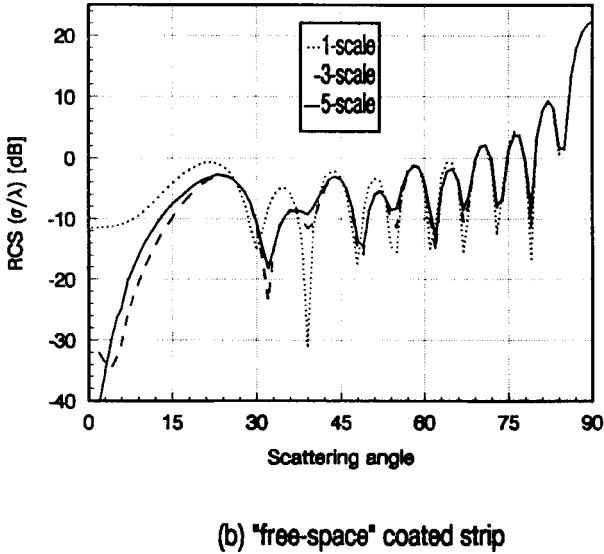
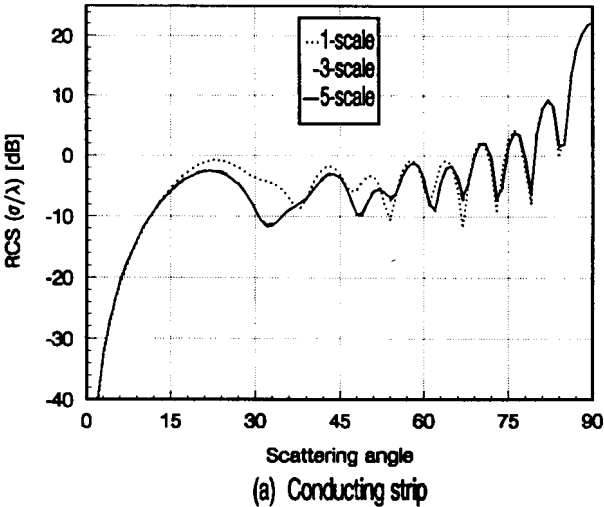


Figure 7. The monostatic RCS for TE case.

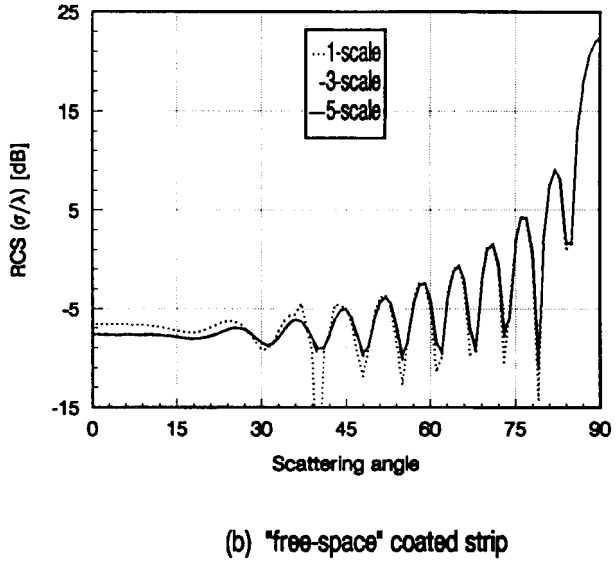
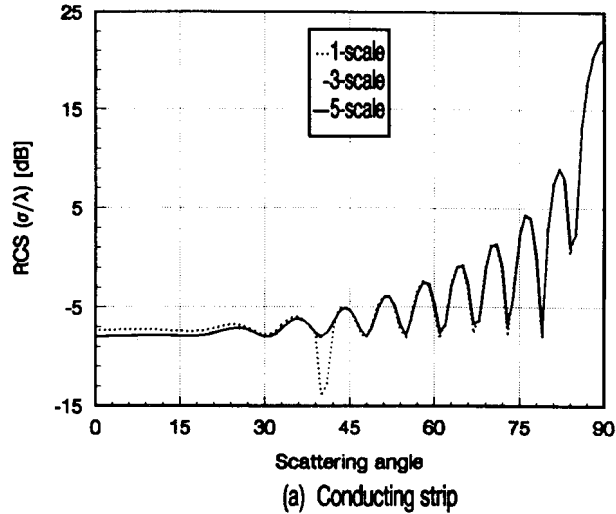


Figure 8. The monostatic RCS for TM case.

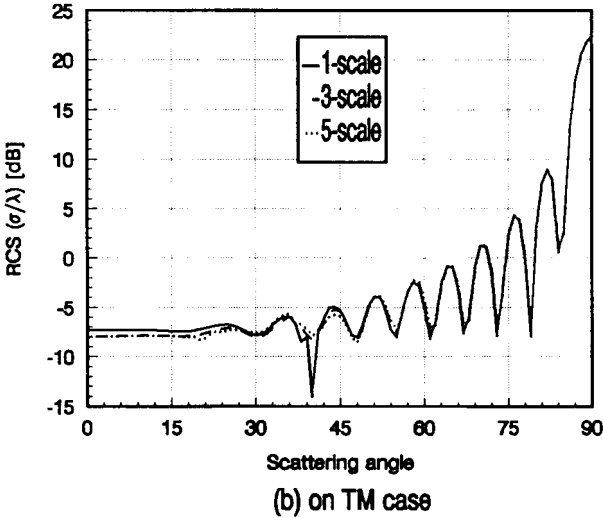
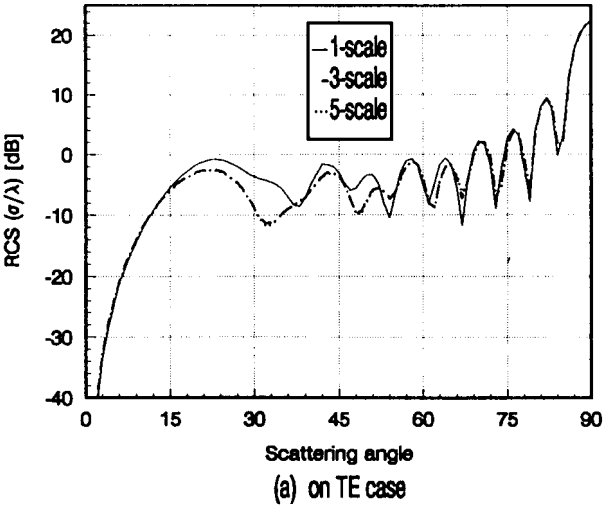
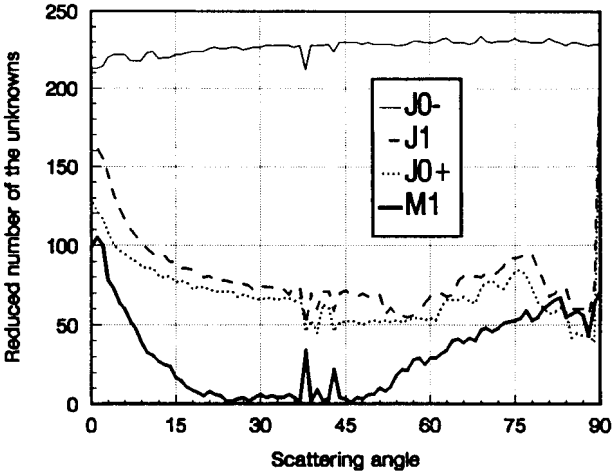
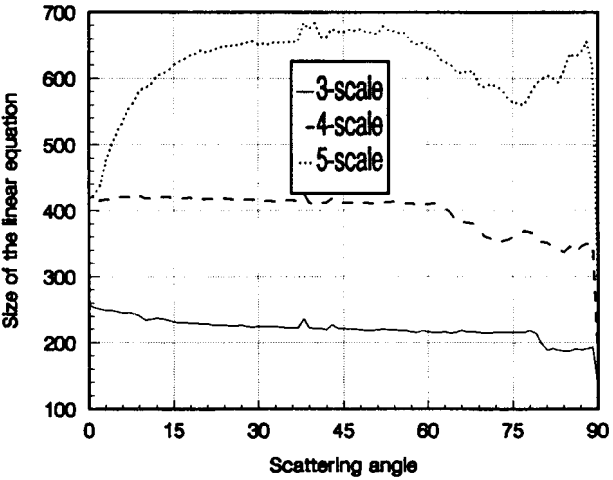


Figure 9. RCS of a computed total current on conducting surfaces.



(a) The reduced number of the unknowns on 5th-scale



(b) The size of the linear equation

Figure 10. Effect of reduced numbers of unknowns through the threshold $\varepsilon = 0.01$ on TM case.

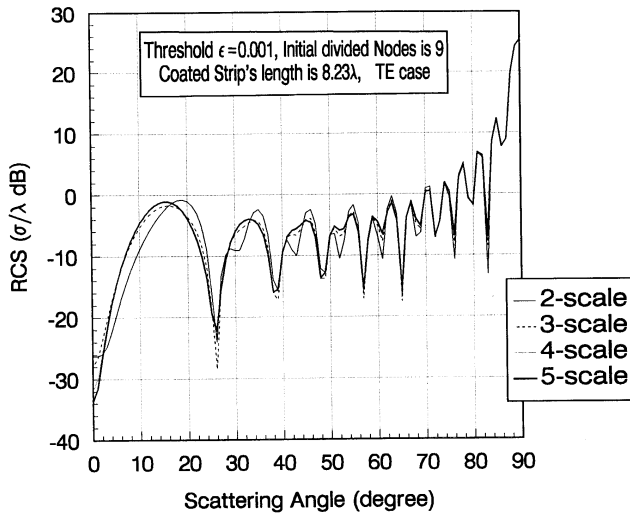


Figure 11. Radar cross sections of coated strip by Adaptive Multiscale Moment Method.

6. CONCLUSION

Electromagnetic scattering from flat coated conducting strips is solved using a combination of a wavelet-like basis functions on different scales. AMMM was presented for analyzing scattering from the coated conducting strip. Many of numerical examples for TM and TE case have been presented. It is shown that the size of the moment matrix can significantly be reduced by utilizing different scale and by setting different thresholds. Numerical results have demonstrated that AMMM is an efficient, adaptive and accurate method.

Application of this approach to the radiating or scattering of the arbitrary geometry in two- or three-dimension is currently under investigation.

ACKNOWLEDGMENT

This work was supported in part by the CASE Center and the E. I. Dupont de Nemours and Company.

REFERENCES

1. Harrington, R. F., *Field Computation by Moment Method*, Macmillan Press, New York, 1968.
2. Medgyesi-Mitschang, L. N., and J. M. Putnam, "Electromagnetic scattering from electrically large coated flat and curved strips: Entire domain Galerkin formulation," *IEEE Trans. Antennas Propagat.*, Vol. AP-35, 790–801, July 1987.
3. Medgyesi-Mitschang, L. N., and D. S. Wang, "Hybrid solutions for scattering from large bodies of revolution with material discontinuities and coatings," *IEEE Trans. Antennas Propagat.*, Vol. AP-32, 717–723, June 1984.
4. Kishk, A. A., A. W. Glisson, P. M. Goggans, "Scattering from conductors coated with materials of arbitrary thickness," *IEEE Trans. Antennas Propagat.*, Vol. AP-40, 108–112, Jan. 1992.
5. Petre, P., M. Swaminathan, G. Veszely, T. K. Sarkar, "Integral equation solution for analyzing scattering from one-dimensional periodic coated strips," *IEEE Trans. Antennas Propagat.*, Vol. AP-41, 1069–1080, Aug. 1993.
6. Petre, P., M. Swaminathan, L. Zombory, T. K. Sarkar, K. A. Jose, "Volume/surface formulation for analyzing scattering from coated periodic strip," *IEEE Trans. Antennas Propagat.*, Vol. AP-42, 119–122, Jan. 1994.
7. Rao, S. M., C. C. Cha, R. L. Cravey, D. L. Wilkes, "Electromagnetic scattering from arbitrary shaped conducting bodies coated with lossy materials of arbitrary thickness," *IEEE Trans. Antennas Propagat.*, Vol. AP-39, 627–631, May 1991.
8. Richmond, J. H., "Digital computer solutions of the rigorous equations for scattering problems", *Proc. IEEE*, Vol. 53, 796–804, Aug. 1965.
9. Mittra, R., (ed.), *Computer Techniques for Electromagnetics*, Pergamon Press, Oxford, 1973.
10. Balanis, C. A., *Antenna Theory: Analysis and Design*, Harper & Row, New York, 1982, 283–321.
11. Bulter, C. M., and D. R. Wilton, "Analysis of various numerical techniques applied to thin-wire scatterers", *IEEE Trans.*, Vol. AP-23, No. 4, 524–540, July 1975.
12. Meyer, Y., *Wavelets: Algorithms & Applications*, translated and revised by R. D. Ryan, SIAM Press, Philadelphia, 1993.
13. Daubechies, I., *Ten Lectures on Wavelet*, SIAM Press, Philadelphia, 1992.
14. Chui, C. K., *An Introduction to Wavelets*, Academic, New York, 1991.

15. Chui, C. K., Ed., *Wavelets- A Tutorial in Theory and Applications*, Academic, New York, 1992.
16. Daubechies, I., "Orthonormal bases of compactly supported wavelets," *Commun. Pure Appl. Math.*, Vol. 41, 909-996, Nov. 1988.
17. Beylkin, G., R. R. Coifman, and V. Rokhlin, "Fast wavelet transform and numerical algorithm I," *Comm. Pure Appl. Math.*, Vol. 44, 141-183, 1991.
18. Steinberg, B. Z., and Y. Leviatan, "On the use of wavelet expansions in method of moments," *IEEE Trans. Antennas Propagat.*, Vol. AP-41, no. 5, 610-619, May 1993.
19. Steinberg, B. Z., and Y. Leviatan, "Periodic wavelet expansions for analysis of scattering from metallic cylinders," *IEEE Antennas Propagat. Soc. Symp.*, 20-23, June 1994.
20. Wagner, R. L., P. Otto, and W. C. Chew, "Fast waveguide mode computation using wavelet-like basis functions," *IEEE Microwave Guided Wave Lett.*, Vol. 3, 208-210, July 1993.
21. Franza, O. P., R. L. Wagner, and W. C. Chew, "Wavelet-like basis functions for solving scattering integral equation," *IEEE Antennas Propagat. Soc. Symp.*, 3-6, June 1994.
22. Kim, H., and H. Ling, "On the application of fast wavelet transform to the integral equation of electromagnetic scattering problems," *Microwave Opt. Technol. Lett.*, Vol. 6, No. 3, 168-173, Mar. 1993.
23. Goswami, J. C., A. K. Chan, and C. K. Chui, "On solving first-kind integral equations using wavelets on a bounded interval," *IEEE Trans. Antenna Propagat.*, Vol. AP-43, No. 6, 614-622, June 1995.
24. Wang, G., "A hybrid wavelet expansion and boundary element analysis of electromagnetic scattering from conducting objects," *IEEE Trans. Antenna Propagat.*, Vol. AP-43, No. 2, 170-178, Feb. 1995.
25. Sarkar, T. K., R. S. Adve, L. Castillo, and M. Palma, "Utilization of wavelet concepts in finite elements for an efficient solution of Maxwell's equations," *Radio Science*, Vol. 29, 965-977, July 1994.
26. Garcia-Castillo, L., M. Salezar-Palma, T. K. Sarkar, and R. S. Adve, "Efficient solution of the differential form of Maxwell's equations in rectangular regions," *IEEE Trans. on MTT*, Vol. 43, No. 3, 647-654, March 1995.
27. Brandt, A., "Multi-level adaptive solutions to boundary value problems," *Mathematics of Computation*, Vol. 31, 330-390, 1977.
28. Hackbusch, W., *Multigrid Methods and Applications*, Springer-Verlag, New York, 1985.

29. McCormick, S. F., *Multigrid Methods: Theory, Applications and Suppercomputing*, Marcel Dekker, New York, 1988.
30. Mandel, J., "On multilevel iterative methods for integral equations of the second kind and related problems," *Numer. Math.*, Vol. 46, 147–157, 1985.
31. Hemker, P. W., and H. Schippers, "Multiple grid methods for the solution of Fredholm integral equations of the second kind," *Mathematics of Computation*, Vol. 36, No. 153, 1981.
32. Kalbasi, K., and K. R. Demarest, "A multilevel enchancement of the method of moments", in *7th Ann. Rev. Progress Appl. Computat. Electromagn.*, Naval, Monterey, CA, 254–263, Mar. 1991.
33. Kalbasi, K., and K. R. Demarest, "A multilevel formulation of the method of moments", *IEEE Trans. Antennas Propagat.*, Vol. AP-41, No. 5, 589–599, May 1993.